

ON Semiconductor

Is Now

onsemi™

To learn more about onsemi™, please visit our website at
www.onsemi.com

onsemi and **onsemi** and other names, marks, and brands are registered and/or common law trademarks of Semiconductor Components Industries, LLC dba "**onsemi**" or its affiliates and/or subsidiaries in the United States and/or other countries. **onsemi** owns the rights to a number of patents, trademarks, copyrights, trade secrets, and other intellectual property. A listing of **onsemi** product/patent coverage may be accessed at www.onsemi.com/site/pdf/Patent-Marking.pdf. **onsemi** reserves the right to make changes at any time to any products or information herein, without notice. The information herein is provided "as-is" and **onsemi** makes no warranty, representation or guarantee regarding the accuracy of the information, product features, availability, functionality, or suitability of its products for any particular purpose, nor does **onsemi** assume any liability arising out of the application or use of any product or circuit, and specifically disclaims any and all liability, including without limitation special, consequential or incidental damages. Buyer is responsible for its products and applications using **onsemi** products, including compliance with all laws, regulations and safety requirements or standards, regardless of any support or applications information provided by **onsemi**. "Typical" parameters which may be provided in **onsemi** data sheets and/or specifications can and do vary in different applications and actual performance may vary over time. All operating parameters, including "Typicals" must be validated for each customer application by customer's technical experts. **onsemi** does not convey any license under any of its intellectual property rights nor the rights of others. **onsemi** products are not designed, intended, or authorized for use as a critical component in life support systems or any FDA Class 3 medical devices or medical devices with a same or similar classification in a foreign jurisdiction or any devices intended for implantation in the human body. Should Buyer purchase or use **onsemi** products for any such unintended or unauthorized application, Buyer shall indemnify and hold **onsemi** and its officers, employees, subsidiaries, affiliates, and distributors harmless against all claims, costs, damages, and expenses, and reasonable attorney fees arising out of, directly or indirectly, any claim of personal injury or death associated with such unintended or unauthorized use, even if such claim alleges that **onsemi** was negligent regarding the design or manufacture of the part. **onsemi** is an Equal Opportunity/Affirmative Action Employer. This literature is subject to all applicable copyright laws and is not for resale in any manner. Other names and brands may be claimed as the property of others.



ON Semiconductor®

<http://onsemi.com>

How to Extend a Thermal-RC-Network Model (Derived from Experimental Data) to Respond to an Arbitrarily Fast Input

Prepared by: Roger Paul Stout, PE and David T. Billings, PE
ON Semiconductor

APPLICATION NOTE

Abstract

For a growing number of customers, transient thermal response of packaged semiconductor devices is a critical issue. It is not enough to predict “time averaged” junction temperatures based on average power dissipation, because the actual duty cycle and associated transient response of a device may lead to peak junction temperatures vastly higher than such steady-state predictions. Experimental techniques exist for accurately measuring the thermal transient response of a physical device in the 100 microsecond range, and thermal RC-networks can readily be generated to match these measurements. Such networks can then be exercised with modeling tools such as SPICE to obtain predictions for time-varying power inputs in this time range. Faster experimental measurements are often complicated by uncontrollable electronic interactions, yet in real-life applications, power cycling of a device may necessitate accurate predictions of the thermal response of the system in the microsecond time frame (or faster). It will be shown that a thermal RC-network model based on experimental data can be readily modified by following straightforward rules, such that an arbitrarily fast response can be accommodated. This concept can also be used to optimize the meshing of 3D finite-element models such that accurate transient response is obtained in the desired time domain, yet model size is minimized.

Glossary of Symbols

R	thermal resistance ($^{\circ}\text{C}/\text{W}$)
C	thermal capacitance ($\text{W}\text{-s}/^{\circ}\text{C}$)
T	temperature ($^{\circ}\text{C}$)
q	energy per area
E	energy
r	size ratio between RC rungs
n	number of sub rungs in the RC network
t	time (seconds)
τ	characteristic time
ρ	density of the solid
c_p	specific heat
k	thermal conductivity
L	element thickness or length
α	thermal diffusivity
u	unit step function
a	pulse width of energy input

INTRODUCTION

Thermal characteristics of packaged integrated circuits and discrete devices have long been a major concern for both manufacturers and users of electronic products. Since reliability is intimately associated with device junction temperature, providing customers with accurate thermal characterization data along with timely product thermal support becomes increasingly critical. One approach by semiconductor manufacturers to transient thermal response has been the “transient thermal response” curve. This curve shows the thermal response of a device over time, given a “step” application of constant power. Using appropriate analytical methods, this curve can be applied to varying power inputs, duty cycles, and waveforms (see AND8219). Measurement techniques supporting the transient response curve are quite complex and have been the subject of numerous papers [1]–[4]. An alternative to the transient response curve is a thermal resistor–capacitor network. With the advent of high-powered network analysis tools, such as SPICE, the RC network is much easier to model for arbitrarily complicated power inputs.

One can view an RC network (a “lumped-parameter” model) as a rather extremely simplified finite element model. While a full-blown, 3D finite element model of a package can be correlated with physical measurements (and in effect “calibrated” against experimental data), the run time can be enormous (especially for transient problems), and finding the “best fit” model to the data is far from a trivial task; further, there are often far too many poorly known parameters which can be arbitrarily adjusted in order to achieve a good fit, for instance, the thermal conductivity of each material in the model, and its associated functional behavior with respect to temperature. Likewise uncertain, but often with significant influence, are interfacial thermal resistances, die attach and encapsulant voiding and anisotropies, and internal or underlying PCB thermal/structural anisotropies, etc. One primary advantage of a simpler lumped-parameter model, therefore, is the manageable number of parameters to be adjusted. Indeed, if these parameters are derived from a best-fit method to the very data which they purport to explain, there is no ambiguity to the choices. Techniques for deriving

RC–ladder networks of semiconductor packages from experimental transient data have been established by one of the authors [5] and others.

The challenge in developing a thermal–RC network for a package is twofold. First, there are measurement limitations that prevent the package from being characterized at the shortest time ranges of interest. When testing “live” devices (which is when one cares the most about accurate thermal data over very short time periods), the process of switching a “heating” power supply off and then switching a “measurement” power supply on, tends to result in large electrical transients in the measured “temperature sensitive parameter.” Unfortunately, this operation is inescapable when the goal is to sense the temperature of the very semiconductor circuit element which dissipates the most significant amount of power in the package. These electrical transients can easily last longer than the interval over which the temperature information is desired, hence reliable experimental data may be unavailable when it is most needed. The second problem with a lumped–RC model (derived from whatever reliable data *is* available), is that intrinsically it can only accurately reproduce thermal behavior of a system at the approximate time constant of its finest–resolution elements (and then only if they are properly located within the model).

In other words, any finite element model (whether lumped RC’s or otherwise) which is derived or calibrated based solely on experimental data, will be fundamentally inaccurate when predicting transient responses for times shorter than those originally measured. It can be tempting to look at a thermal transient curve which shows no “significant” temperature change between the first 100 and 500 microseconds, then to derive an RC network model which fits the existing data “perfectly” and has a 200 microsecond time constant, and *then* to presume that this RC model can be used to accurately model the junction temperatures with a 10 microsecond duty cycle. “After all,” one reasons, “we saw effectively no temperature change until after 500 microseconds, so a 200 microsecond response time must be adequate.” (Wrong!)

To understand this deficiency, we must first study the physical/mathematical basis of the substantial difference in transient behavior (at the shortest times) between a lumped parameter model and a “distributed” parameter model. Since the real world of semiconductor thermal physics is a material continuum, this distinction is paramount. It can be illustrated by exploring a simple system and observing the magnitude of the errors which can result when the incorrect (lumped) model is used. Then, this same “incorrect” model will be modified such that it becomes more accurate for shorter times, and an algorithm presented to guide such modifications accurately to arbitrarily short times. Finally, this process will be demonstrated using a full set of typical experimental data.

Discrete vs. Continuous Heat Transfer Physics

The “real world” consists of regions of reasonably continuous material properties; the boundaries between the regions also may have their own particular properties. When the response of a region as a whole can be suitably treated, it may be considered as a “lump”, but if we are interested in internal details, it may be necessary to treat it like a continuous distribution of matter.

For example, suppose a semiconductor package has a total mass of five grams, and is comprised of materials with (on the average) a specific heat capacity of something like $1.2 \text{ W} \cdot \text{s}/\text{gm} \cdot ^\circ\text{C}$. Its thermal capacitance (the “C” part of the RC model) is therefore something like $6 \text{ W} \cdot \text{s}/^\circ\text{C}$ (the product of mass times specific heat). Also suppose that according to steady state measurements on a certain circuit board, it has a thermal resistance of perhaps $25^\circ\text{C}/\text{W}$ (the “R” part). Its lumped–parameter thermal time constant is therefore something like 150 seconds (the product of R and C). If we are interested in knowing how long it will take, from the time we first apply power to the package, until the package itself has reached some sort of thermal equilibrium, this single RC time constant model is entirely reasonable. Further, estimates of average junction temperature will be valid for any sort of power duty cycle which changes less often than, say, every five minutes. For instance, at an average power dissipation of 1.0 W, the “steady” junction temperature will be 25°C above the board (case) temperature.

But what if the power is applied with a 1% duty cycle of 10 milliseconds on (at 100 W), then 990 milliseconds off, etc., to sustain that average power level of 1.0 W? We know that the silicon inside the package (where the heat originates) has a total mass of 0.07 gm (a $10 \times 10 \times 0.3$ mm chip), and a heat capacity of $0.67 \text{ W} \cdot \text{s}/\text{gm} \cdot ^\circ\text{C}$, for a thermal capacitance of $0.047 \text{ W} \cdot \text{s}/^\circ\text{C}$. Assuming that the power is dissipated uniformly on one surface of the chip and that the bulk of this heat passes through the chip to the leadframe underneath (as opposed to exiting through the poorly conducting encapsulant above), the thermal resistance of this path will be about $0.03^\circ\text{C}/\text{W}$ (length over area over conductivity). Thus the “lumped” response time of the chip within the package is about 1.4 millisecond, much shorter than the “on” time of the power cycle. 100 W applied for 0.01 sec is $1.0 \text{ W} \cdot \text{s}$ of energy, so the temperature rise of the junction (as compared with the back side of the chip) could be as high as $1.0/0.047$, or 21°C (depending on how quickly the heat can escape from the chip. Yes, the *average* junction temperature will still be but 25°C higher than the case, but the peak rise could be nearly twice as high over ambient as the average value. Clearly, our first “single lump” package model was inadequate to predict this result (though unwise to even try, based on the timescale of interest, we would have computed $1.0/6 = 0.2^\circ\text{C}$); but we only know that we fall short by two orders of magnitude, because we have the ability and have taken the trouble to estimate what could be happening at a finer detail of the package geometry.

What, then, if the power duty cycle has an “on” period of 10 *microseconds*? It would be prudent to be cautious of even the lumped “chip scale” model, as we shall see.

Simple Models

Comparison of Simplest Models

Without belaboring the mathematics behind the following equations, we can answer the preceding question fairly quickly by examining a specific, “special case.” The following equations describe the time–domain response to a square–edged power pulse (of finite width and amplitude), delivering a total energy E, for each of three physical models.

The first equation describes the response of a single lumped–parameter system (i.e., one R, one C, just as we have been exploring already). It may be recognized as a simple exponential response to a “step” input, complicated only by the addition of the delayed “un–step” to remove the applied power after the specified pulse width. (The u function is the “unit step” function which is defined to be zero when the argument is negative, and unity when the argument is non–negative.)

The second equation is the exact solution for a distributed material domain of finite thickness (and heat input is uniform per unit area on one boundary), where the “output” boundary of the domain is at thermal ground. This is the simplest possible continuous domain problem corresponding to a finite, single–lump RC.

The third equation is the response of a semi–infinite continuous domain (to a uniform flux on the input boundary). It is presented to help clarify the difference between the first two models. We would expect this third model to act just like the “correct” finite–extent model (Equation 2) for short enough times (i.e., well before the heat pulse reaches the “ground” side of the domain), but would not expect it to match the behavior as time gets large. Because it is functionally so much simpler than the “exact” model, however, it will be much easier to understand the difference between it and the lumped RC model at those short times.

For the lumped RC model, a finite volume of material with a particular thermal capacitance makes sense, and the energy input is sensibly treated in units of energy. For the finite–extent distributed model, it is fortuitous that the RC product happens to be independent of the area normal to the heat flow, and therefore the energy and capacitance can be treated either in their “natural” units, or in “per area” units. For the semi–infinite distributed model, neither energy nor capacitance make any sense unless viewed on a “per area” basis, but because there is no characteristic length, neither do the concepts of capacitance per area, nor characteristic time. Conveniently, however (because we seek to compare this model’s response to the others), if we introduce the characteristic length and time from the other models, it happens to result in the same quantities of energy and capacitance (converting the input energy/area, q, into an energy, E).

Thus, Equations 1, 2, and 3, all can be rewritten by normalizing the time (now t’ and a’) with respect to the characteristic time of the RC model (which is the same as that of the finite extent model), and by normalizing the temperature by the quantity C_{th}/E. Equations 4, 5, and 6 are the corresponding non–dimensionalized versions for the three models. Figure 1 is a plot of the peak temperature reached (namely, at time t = a, or t’ = a’) by the “junction” (where the heat is input) of each of the three models as a function of the pulse width (a’ = 1 when the pulse width is equal to the characteristic time). As expected, when the pulse is very short with respect to the characteristic time (that is, the pulse ends long before the heat can propagate to the far side of the region), Equations 5 and 6 (the finite–extent and semi–infinite distributed models) agree precisely. When the pulse is very long with respect to the characteristic time, it shows the expected agreement between Equations 4 and 5 (the lumped and finite–extent models), while the semi–infinite solution diverges.

Dimensional Equations

$$T(t)_{\text{pulse lumped-RC}} = \frac{E}{C_{th} a} \tau \left[\left(1 - e^{-\frac{t}{\tau}} \right) - u(t-a) \left(1 - e^{-\frac{(t-a)}{\tau}} \right) \right] \tag{eq. 1}$$

$$T(t)_{\text{pulse finite-extent}} = \frac{E}{C_{th} a \sqrt{\pi}} \left\{ \sqrt{\frac{t}{\tau}} \left[1 + 2 \sum_{n=1}^{\infty} (-1)^{-n} \left[e^{-\frac{n^2 \tau}{t}} - n \sqrt{\frac{\pi \tau}{t}} \operatorname{erfc} \left(n \sqrt{\frac{t}{\tau}} \right) \right] \right] \right. \\ \left. - \sqrt{\frac{t-a}{\tau}} \cdot u(t-a) \left[1 + 2 \sum_{n=1}^{\infty} (-1)^{-n} \left[e^{-\frac{n^2 \tau}{t-a}} - n \sqrt{\frac{\pi \tau}{t-a}} \operatorname{erfc} \left(n \sqrt{\frac{t-a}{\tau}} \right) \right] \right] \right\} \tag{eq. 2}$$

$$T(t)_{\text{pulse semi-infinite}} = \frac{2q}{a \sqrt{\rho c_p k \pi}} \left[\sqrt{t} - u(t-a) \sqrt{t-a} \right] \tag{eq. 3}$$

Non-Dimensional Equations

$$\frac{C_{th}}{E} T(t)_{\text{pulse lumped-RC}} = \frac{1}{a'} [(1-e^{-t'}) - u(t-a')(1-e^{-(t'-a')})] \tag{eq. 4}$$

$$\frac{C_{th}}{E} T(t)_{\text{pulse finite-extent}} = \frac{2}{a' \sqrt{\pi}} \left\{ \sqrt{t'} \left[1 + 2 \sum_{n=1}^{\infty} (-1)^{-n} \left[e^{-\frac{n^2}{t'}} - n \sqrt{\frac{\pi}{t'}} \operatorname{erfc}\left(\frac{n}{\sqrt{t'}}\right) \right] \right] \right. \\ \left. - \sqrt{t'-a'} \cdot u(t-a) \left[1 + 2 \sum_{n=1}^{\infty} (-1)^{-n} \left[e^{-\frac{n^2}{t'-a'}} - n \sqrt{\frac{\pi}{t'-a'}} \operatorname{erfc}\left(\frac{n}{\sqrt{t'-a'}}\right) \right] \right] \right\} \tag{eq. 5}$$

$$\frac{C_{th}}{E} T(t)_{\text{pulse semi-infinite}} = \frac{2}{a' \sqrt{\pi}} \left[\sqrt{t'} - u(t-a) \sqrt{t'-a'} \right] \tag{eq. 6}$$

What may be surprising is how very much higher the peak temperature is for the “correct” (i.e., continuous media) models versus the lumped RC model, when the pulse is short compared to the time constant of the model. If the pulse is only 1/100th the length of the RC time constant, the actual temperature rise is more than an order of magnitude larger than that predicted. This error ratio grows as the square root of the pulse width ratio, or precisely;

$$\frac{\text{correct (distributed)}}{\text{lumped RC}} = \frac{2}{\sqrt{\pi}} \sqrt{\frac{\tau}{a}} \tag{eq. 7}$$

As an aside, note that in a strict sense, the term “time constant” should only be applied to the RC model; the term “characteristic time” is more appropriate for the other models. Though this “characteristic time” conveys a similar meaning (namely, that the energy takes something on the order of that time to traverse the region, or that it takes on that order of time to reach a significant fraction of its final value), it does not follow the more familiar exponential rules of 63% after one time constant, and so forth. (In fact, in response to a step input, the finite-extent model reaches 93% of its final value after only one characteristic time.)

Enhanced RC Model

Hopefully, it is now clear that a 1-rung RC model is incapable of accurately predicting transient behavior for a continuous medium, when the desired predictions are for times much shorter than the lumped-parameter time constant of the system. If we had observed this problem while building a 3D finite element model (FEM) of the package, at this point we would have said simply “increase the mesh density!” (Though one important point being made here is that unless the user is paying careful attention, the observation that the smallest elements of the FEM were too large might not even have been made!) Except for our choice of mesh size, we would have no direct concern over the new values of the R’s and C’s computed by the modeler – it would take care of it for us transparently. What we have done by refining the mesh, however, is simply to subdivide the existing elements into smaller pieces. Total system capacitance is not changing, and total system resistance over the same path length in any particular direction isn’t

changing. We can do exactly the same thing with our 1-D, 1-rung model, by dividing the R and C into proportionally sized sub-elements.

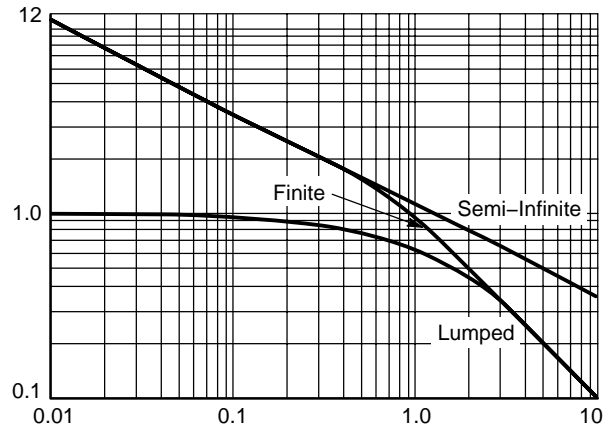


Figure 1. Normalized peak response to finite pulses for finite-extent, semi-infinite, and lumped parameter models as a function of normalized pulse width.

To clarify the concept, first suppose that we simply divide the single-rung RC network into a two-rung ladder (as illustrated in Figures 2 and 3), such that the overall resistance and capacitance of the system are conserved. If r is the relative size ratio between the two rungs, then the specific relationship between the rungs and elements of the two ladders is as shown. It should be fairly clear how the r ratio has been applied simply and directly to the capacitances, but perhaps less so with respect to the resistances. To understand the resistances, observe that the same fractions of the total resistance are computed, but that the fraction corresponding to the lower rung has been divided in two and split across the two resistance elements in the ladder. This is because the path resistance *between* any two nodes is attributed half to the material associated with each of them (just as if this were indeed a finite element model), whereas the capacitance is associated directly with each node and represents the thermal mass of the node itself.

Because there is only one path away from the “junction” node, its entire share (not half) of resistance is included there. Since the total resistance adds up to the original R, the “DC limit” of these two networks will be the same.

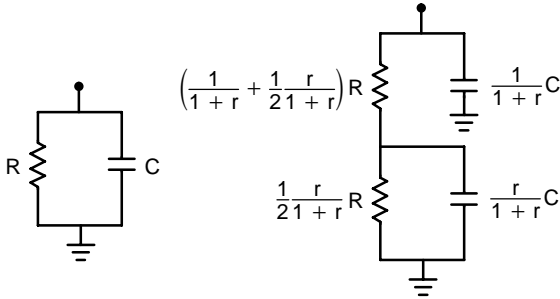


Figure 2. 1-Rung Model Figure 3. 2-Rung Model

We can generalize this concept fairly easily to any number of rungs, where as we move farther and farther from the junction node, each rung is the same fixed size ratio r larger than the preceding rung. The only complication (as compared to the 2-rung version) is that to conserve the total capacitance and resistance, the equations get more complex. If the number of rungs desired is n , Equation 8 tells us how to compute the fractional size of the smallest rung, such that when we sum the sizes of all the elements in the network, they will add up to the original single-lump model values.

$$C_1 = \frac{r-1}{r^{n-1}}C, C_2 = rC_1, C_3 = rC_2, \text{ etc. (eq. 8)}$$

The resistances will follow exactly the same relative ratios, but again, each resistance (except the junction element's) will be split equally between adjacent nodes. Figure 4 shows such a four-rung network.

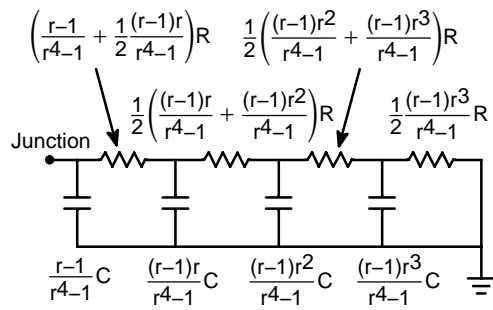


Figure 4. A Four-Rung, Fixed-Ratio Ladder

To see what is the effect on the pulse response of this modification to the model, it will be instructive simply to consider how the circuit responds to a step. First, in all of Figures 5 through 7, note that the “exact solution” (the finite-extent, continuous domain step response) has a log-log slope of 1:2 below the “characteristic time” (a direct consequence of the square-root of time behavior). By contrast, every lumped-parameter model, if it is extended to times shorter than its fastest-rung time constant, ends up at a log-log slope of 1:1. As the time of interest gets much smaller than the model can resolve, the relative error will get larger (as we have already discovered).

Figure 5 illustrates that with four rungs, once the size ratio gets larger than about 4:1, a distinct “waviness” appears in the response. Also, there is considerable “overshoot” in the response (i.e., higher amplitude than the exact solution) once into the 1:2 slope region. Figure 6 confirms that the “waviness” is a problem at a ratio of 16:1 regardless of the number of rungs chosen. Figure 7 illustrates that at a fixed rung-to-rung size ratio of 3:1, every addition of 1 rung extends the range of the 1:2 slope region faster, by essentially one order of magnitude; further, there is no perceptible waviness in the response, and the overshoot is negligible.

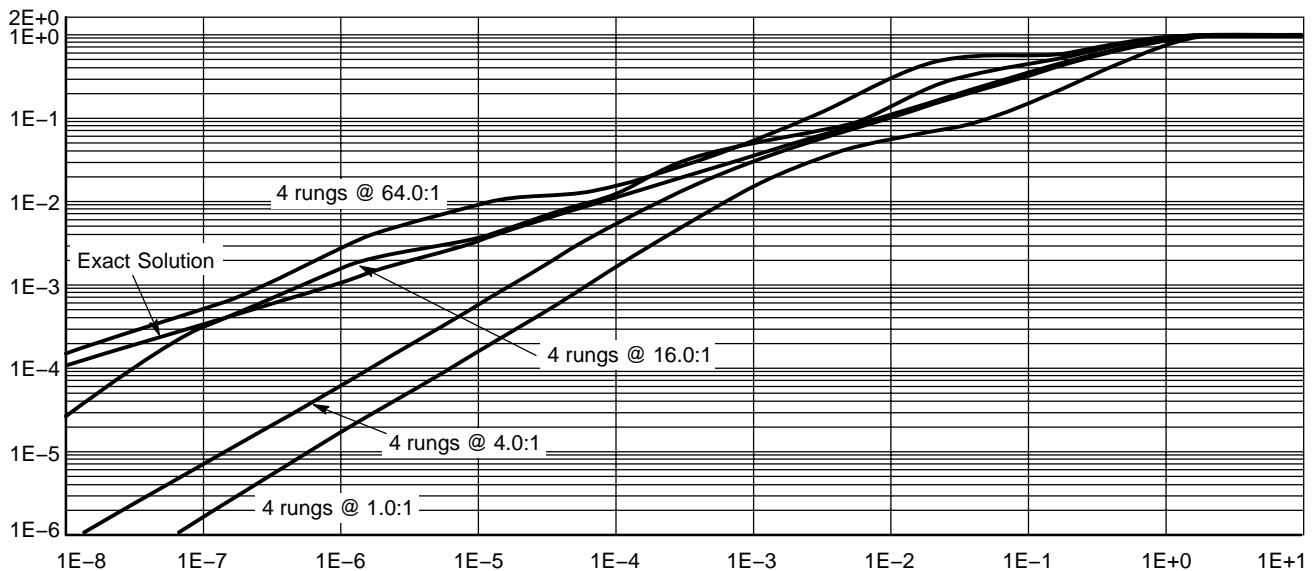


Figure 5. Step Response of 4 Rung Networks with Differing Element Size Ratios

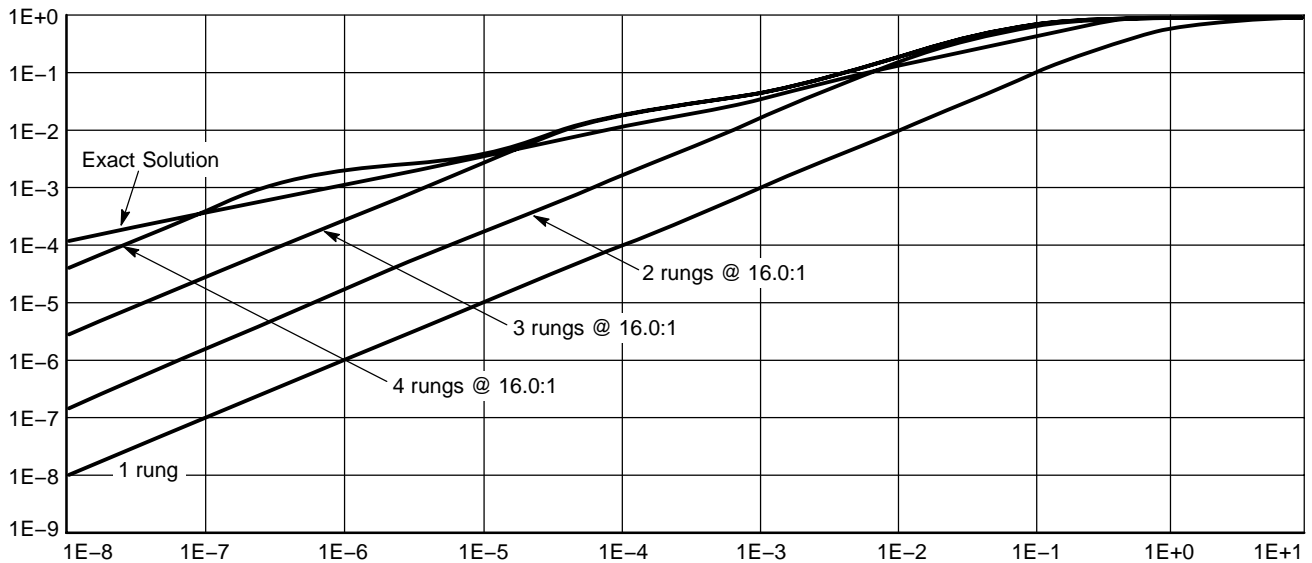


Figure 6. Step Response of 1-4 Rung Networks with Progressive Element Size Ratio of 16

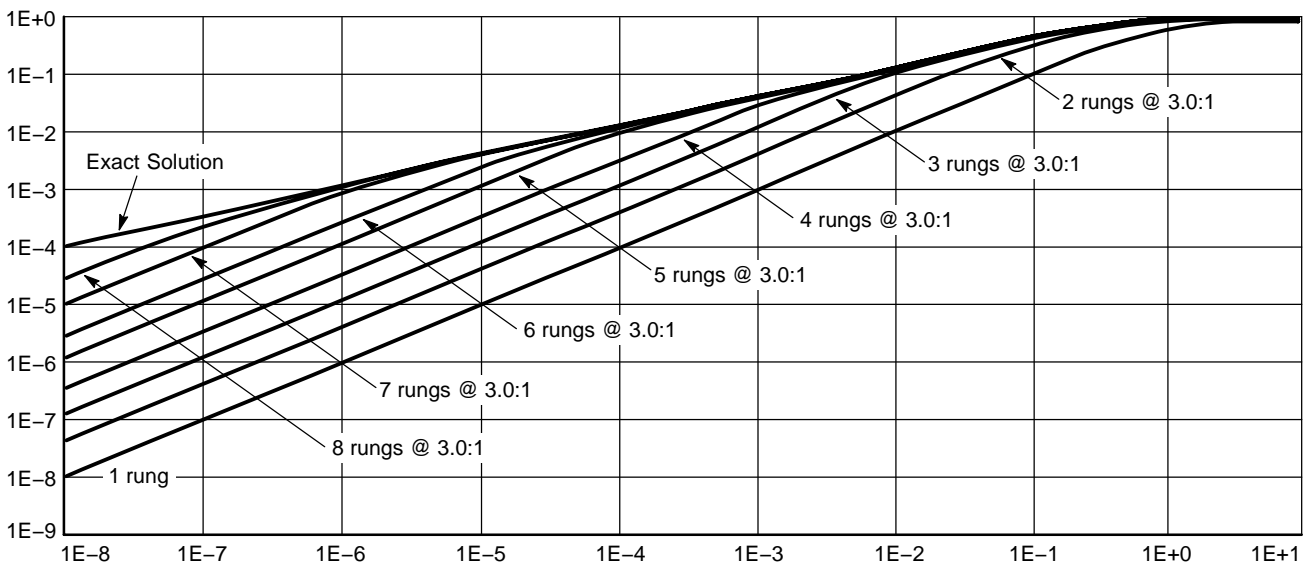


Figure 7. Step Response of 1-8 Rung Networks with Progressive Element Size Ratio of 3.0

The Algorithm

Based on the foregoing analysis, the following rules are recommended for extending the fast-time response of RC-network models derived from experimental data:

1. Identify the fastest response time for which the experimental data is reliable.
2. Fit a minimal-rung RC network to that data, such that the response of the fastest element is not faster than that range (and satisfies any other accuracy requirements at all longer times). If the data clearly enters a 1:2 log-log slope region, be sure that the “best fit” network is able to match the “slowest” part of that range (though it need not necessarily match the fastest data well).

3. Knowing the fastest power cycling which will be applied to the device in real life (if faster than the network already obtained), count the additional number of orders of magnitude of response needed. This plus one (Equation 9), will be the number of sub-rungs, n, into which the best-fit’s fastest rung must be subdivided.

$$n = \text{int}(\log_{10}(\tau_{\text{min}}) - \log_{10}(\tau_{\text{desired}})) + 1 \quad (\text{eq. 9})$$

4. The capacitance to be subdivided is simply the capacitance of the fastest rung of the best fit network. Using an element ratio of 3 for r, Equation 8 can be reformulated to compute all the new sub-rungs’ capacitances (Equation 10).

$$C_i = \frac{2 * 3^{(i-1)}}{3^{n-1}} C_{\text{Original fastest}} \quad (\text{eq. 10})$$

5. Because physically the resistances represent material which spans the space between nodes (rather than material lumped at the nodes), the subdivision of the R's is more complicated than for the C's. Equations 11 thru 14 show how to do this for a rung ratio of 3.

$$R_s = \frac{C}{C + C_0} R_{\text{original fastest}} \quad (\text{eq. 11})$$

If $i = n$ then:

$$R_n = (R_{\text{original fastest}} - R_s) + \frac{3(n-1)}{3^n - 1} R_s \quad (\text{eq. 12})$$

If $1 < i < n$ then:

$$R_i = \frac{3^i + 3(i-1)}{3^n - 1} R_s \quad (\text{eq. 13})$$

If $i = 1$ then:

$$R_1 = \frac{5}{3^n - 1} R_s \quad (\text{eq. 14})$$

where C is the capacitance of the original rung being subdivided, and C₀ is the capacitance of the adjacent (slower) rung. [Note that in the original 1-rung ladder used to develop the method, (Figure 2) there was no such slower rung.] A careful comparison of Figures 10 and 11 with Figure 9 (in the following "real-device" example) will hopefully make the R-subdivision method clear.

Real-Device Example

A typical experimental transient response curve (a 6-lead SOT23L plastic package) is shown in Figure 8, along with the original 6-rung "best fit" RC network response (before extension) in Figure 9. Also shown are two additional RC network responses, obtained by applying the algorithm just described to the top rung, first dividing it into two pieces (Figure 10), and then into six (Figure 11). Note that the original junction-rung's 5.52°C/W resistor is partitioned into 4.94 and 0.58°C/W pieces, based on the

0.000455/0.00388 capacitance ratio between the junction rung and the next rung (Equation 11). Only the 0.58°C/W portion is then subdivided into the faster-response added rungs (Equations 12 thru 14).

Application to 3-D Finite Element Models

Since this algorithm (especially the method of handling the resistances) was developed according to the very principles which guide the computation of the nodal capacitances and interconnect resistances of a typical 3-D finite element code, it should be clear that the same conclusions regarding smoothness of response in the 1:2 log-log slope region, and the relationship between size ratio, number of elements, and faster time response capability are applicable. Further, it is much simpler in that the FEM code will take care of the calculations, once you have specified the element dimensions. The crucial feature of a 3-D model is that an element's "characteristic time" is equal to the square of its thickness (in the direction of heat flow) divided by the thermal diffusivity of the material.

$$\tau = \frac{L^2}{\alpha} \quad (\text{eq. 15})$$

You calculate the smallest element thickness necessary to obtain the desired response, apply this value only to the elements directly adjacent to the model's heat source (the chip surface, for instance), and the elements' thickness can grow at a 3:1 ratio moving away from this region until the size is constrained by other model requirements.

CONCLUSION

Based on our experience, the methods presented here can be used to predict accurate thermal transient response to arbitrarily fast power input in an RC thermal network. The initial RC network can be systematically enlarged to encompass the desired time response. These methods also apply in sizing elements of an FEM model to achieve optimum time response in a transient simulation.

AND8218/D

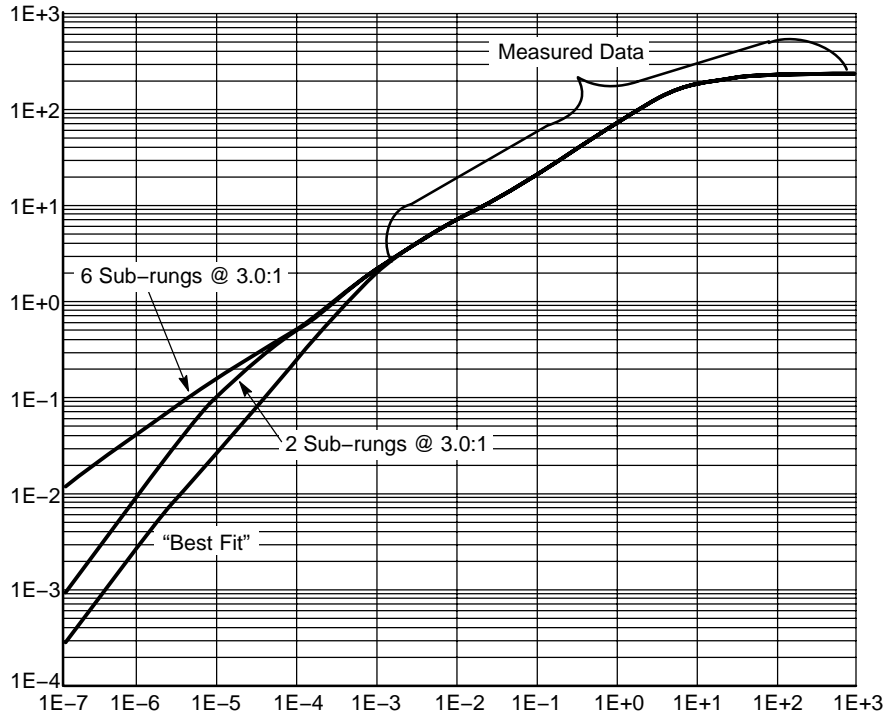


Figure 8. Typical Experimental Data and Resulting RC Network Responses

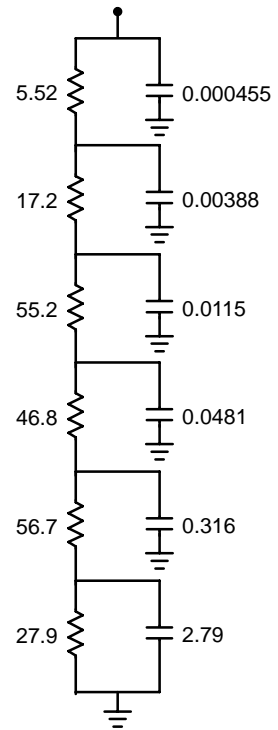


Figure 9. 6-Rung "Best Fit" RC Network (2 ms Resolution)

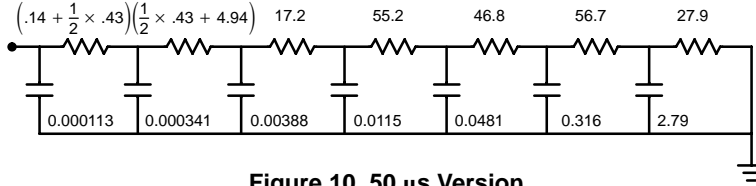


Figure 10. 50 μs Version

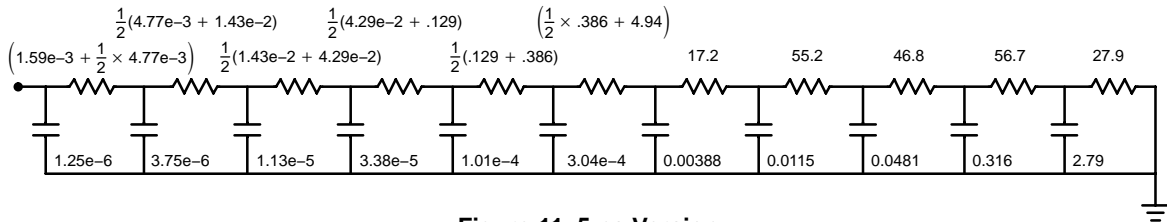



Figure 11. 5 ns Version

References

1. D.L. Blackburn, "An Electrical Technique for the Measurement of the Peak Junction Temperature of Power Transistors," *Annual Proceedings of Reliability Physics*, 1975.
2. D.L. Blackburn and F.F. Oettinger, "Transient Thermal Response Measurements of Power Transistors," Power Electronics Specialists Conference, 1974.
3. P. Antognetti, G.R. Bisio, F. Curatelli, and S. Palara, "Three-Dimensional Transient Thermal Simulation," *IEEE Journal of Solid State Circuitry*, June 1980.
4. S. Clemente, "Transient Thermal Response of Power Semiconductors to Short Power Pulses," *IEEE Transactions on Power Electronics*, October 1993.
5. R.P. Stout, B.A. Zahn, "Application of Thermal Resistor-Capacitor Networks for the Analysis of Transient Junction Temperatures in Semiconductor Packages," *Motorola Summer AMT Symposium*, 1995.

ON Semiconductor and  are registered trademarks of Semiconductor Components Industries, LLC (SCILLC). SCILLC reserves the right to make changes without further notice to any products herein. SCILLC makes no warranty, representation or guarantee regarding the suitability of its products for any particular purpose, nor does SCILLC assume any liability arising out of the application or use of any product or circuit, and specifically disclaims any and all liability, including without limitation special, consequential or incidental damages. "Typical" parameters which may be provided in SCILLC data sheets and/or specifications can and do vary in different applications and actual performance may vary over time. All operating parameters, including "Typicals" must be validated for each customer application by customer's technical experts. SCILLC does not convey any license under its patent rights nor the rights of others. SCILLC products are not designed, intended, or authorized for use as components in systems intended for surgical implant into the body, or other applications intended to support or sustain life, or for any other application in which the failure of the SCILLC product could create a situation where personal injury or death may occur. Should Buyer purchase or use SCILLC products for any such unintended or unauthorized application, Buyer shall indemnify and hold SCILLC and its officers, employees, subsidiaries, affiliates, and distributors harmless against all claims, costs, damages, and expenses, and reasonable attorney fees arising out of, directly or indirectly, any claim of personal injury or death associated with such unintended or unauthorized use, even if such claim alleges that SCILLC was negligent regarding the design or manufacture of the part. SCILLC is an Equal Opportunity/Affirmative Action Employer. This literature is subject to all applicable copyright laws and is not for resale in any manner.

PUBLICATION ORDERING INFORMATION

LITERATURE FULFILLMENT:

Literature Distribution Center for ON Semiconductor
 P.O. Box 61312, Phoenix, Arizona 85082-1312 USA
Phone: 480-829-7710 or 800-344-3860 Toll Free USA/Canada
Fax: 480-829-7709 or 800-344-3867 Toll Free USA/Canada
Email: orderlit@onsemi.com

N. American Technical Support: 800-282-9855 Toll Free
 USA/Canada

Japan: ON Semiconductor, Japan Customer Focus Center
 2-9-1 Kamimeguro, Meguro-ku, Tokyo, Japan 153-0051
Phone: 81-3-5773-3850

ON Semiconductor Website: <http://onsemi.com>

Order Literature: <http://www.onsemi.com/litorder>

For additional information, please contact your local Sales Representative.